

# The drying tendency of shallow meridional circulations in monsoons

Jun Zhai\* and William R. Boos

Department of Geology and Geophysics, Yale University, New Haven, CT, USA

\*Correspondence to: J. Zhai, 210 Whitney Av, New Haven, CT 06511, USA. E-mail: jun.zhai@yale.edu

Shallow meridional overturning circulations are superimposed on the deep circulations that produce precipitation in nearly all monsoon regions, and these shallow circulations transport subtropical, mid-tropospheric dry air into the tropical monsoon precipitation maxima. Here horizontal moisture advection produced by shallow meridional circulations is characterized in the monsoon regions of West Africa, South Asia, Australia, and southern Africa during local summer. Horizontal flow in the upper and lower branches of the shallow meridional circulations consistently dries and moistens air, respectively, in the continental precipitation maxima of each region. The peak drying by horizontal advection occurs at a lower altitude than peak winds in the upper branch of the shallow circulations, consistent with the small scale height of water vapour. Advection of time-mean moisture by time-mean wind dominates horizontal moisture advection in South Asia and West Africa, while most horizontal moisture advection in Australia and southern Africa is produced by transient eddies. Much of the transient eddy advection can be accurately represented as a first-order horizontal diffusion with a constant, globally uniform diffusivity. These results suggest that horizontal moisture advection in theoretical and conceptual models of seasonal mean monsoons can be adequately represented in terms of time-mean winds plus a simple horizontal moisture diffusion. Finally, interannual variations in the summer mean regional averages of monsoon precipitation and horizontal advective drying in the lower free troposphere are shown to be negatively correlated in most regions, consistent with the hypothesis that advective drying by shallow meridional circulations inhibits monsoon precipitation.

*Key Words:* shallow meridional circulations; monsoons; tropical dynamics; eddies; drying tendency

*Received 16 December 2016; Revised 25 May 2017; Accepted 7 June 2017; Published online in Wiley Online Library*

## 1. Introduction

The full vertical distribution of atmospheric moisture exerts a profound influence on tropical precipitation. Traditionally, near-surface moisture has been most closely associated with the readiness of an atmospheric column to precipitate because the humidity and temperature of air parcels below the lifted condensation level determine the amount of potential energy available for moist convection. More recently, the ability of mid-tropospheric dry air to inhibit precipitation has been appreciated. Precipitation, the depth of convective clouds, and the net upward convective mass flux have all been shown to be highly sensitive to dry air above the base of cumulus clouds, in both observations (e.g. Austin and Fleisher, 1948; Sherwood, 1999; Yoneyama and Parsons, 1999; Holloway and Neelin, 2009) and numerical simulations (e.g. Tompkins, 2001; Derbyshire *et al.*, 2004). Time tendencies of lower- and middle-tropospheric humidity due to non-convective processes – principally surface evaporation and advection by large-scale flow – can thus strongly influence the distribution of tropical precipitation.

The horizontal advection of humidity has been shown to be of particular importance in governing the intensity and structure of

monsoon precipitation. Chou *et al.* (2001) showed that advection of cold and dry extratropical air into monsoon regions inhibits monsoon precipitation and limits the poleward expansion of monsoons during local summer. Orography was argued to create a strong South Asian monsoon by suppressing the penetration of dry, low-energy extratropical air into the monsoon thermal maximum (Chakraborty *et al.*, 2006; Boos and Kuang, 2010). More recent work has emphasized that it is the horizontal advection of hot and dry desert air rather than cold and dry extratropical air that would inhibit South Asian rainfall in the absence of orography (Boos and Hurley, 2013; Boos, 2015). Most of these studies of horizontal moisture advection in monsoons have focused on near-surface humidity (e.g. Privé and Plumb, 2007; Nie *et al.*, 2010) or have assumed that the entire vertical distribution of humidity increases with the near-surface humidity (Neelin and Zeng, 2000).

Indeed, monsoons are commonly thought of as deep overturning circulations that can be fully described by a first baroclinic mode structure having convergence in the lower and middle troposphere and divergence in the upper troposphere. Specifically, air ascends in the summer monsoon region, flows across the Equator, and subsides in the winter hemisphere (e.g. Peixoto

and Oort, 1992). However, recent work has shown that shallow circulations also exist in the lower and middle troposphere in nearly all monsoon regions. In these shallow circulations, air ascends in the lower troposphere at least 500 km poleward of the monsoon precipitation maximum, then flows toward the Equator in the middle troposphere, typically in the 500–800 hPa layer (Kawamura *et al.*, 2002; Zhang *et al.*, 2008). The low-level flow that feeds the time-mean ascent in these shallow meridional circulations (SMCs) is superimposed, in the planetary boundary layer, on the low-level inflow to the deep, precipitating monsoon circulation. An SMC in the tropical East Pacific has some similarities to the SMCs observed in monsoon regions, except that in the East Pacific the ascent branch of the SMC is collocated with the ascent branch of the deep, precipitating circulation (Zhang *et al.*, 2004; Nolan *et al.*, 2007). In contrast, ascent in monsoon SMCs typically occurs over the deserts that lie poleward of the deep, precipitating ascent (e.g. Nie *et al.*, 2010). In an empirical decomposition of global monsoon winds in an atmospheric reanalysis, Trenberth *et al.* (2000) found that the first baroclinic deep mode accounted for 60% of the seasonal cycle variance of divergent flow, while a shallow mode accounted for 20% of that variance.

These shallow circulations have been argued to influence monsoon precipitation through advection of moisture, with most studies of this effect focusing on the West African monsoon. The lower branch of an SMC in a monsoon region transports relatively cool and moist air poleward across the precipitation maximum, producing near-surface cooling and moistening poleward of that precipitation maximum via horizontal advection. This has been argued to help shift the West African precipitation maximum northward in the early summer phase of its seasonal cycle (Thorncroft *et al.*, 2011). At the same time, the upper branch of the SMC transports hot, dry air toward the Equator, warming and drying the precipitation maximum in the lower to middle troposphere. The horizontal advective tendencies produced by the West African SMC thus form a vertical dipole, with cooling and moistening in the lowest 1–2 km of the atmosphere over the Sahel and Sahara, and warming and drying above that up to about 5 km (Peyrillé and Lafore, 2007). Zhang *et al.* (2008) suggested that the mid-level advective warming and drying prevents the West African precipitation maximum from shifting northward during early summer, allowing a later abrupt northward jump when sufficient convective instability has accumulated (also Sultan and Janicot, 2000; Gu and Adler, 2004). Similarly, Xie *et al.* (2010) used field campaign data to show that mid-level drying due to horizontal advection contributed to the limited vertical growth of clouds over northern Australia during suppressed episodes of that region's local summer monsoon. Yet another example was discussed by Parker *et al.* (2016), who showed that monsoon onset over South Asia is coincident with the weakening of mid-level dry advection by northwesterlies over India; they argued that this mid-level dry advection suppresses moist convection and causes the onset of monsoon rains to occur earlier in southeastern India than in northwestern India.

Near-surface moistening and mid-level drying by SMCs have thus been argued to alter the onset and subseasonal variability of monsoons in contrasting ways, and the same is true for their effect on seasonal mean monsoon precipitation. Haarsma *et al.* (2005) and Biasutti *et al.* (2009) found a negative correlation between summer-mean Sahel precipitation and low-level geopotential height (or surface pressure) over the Sahara, and argued that this indicated a stronger SMC was causing increased Sahel rainfall by drawing more moisture in from the ocean. However, Shekhar and Boos (2016) showed that the overturning circulation of the West African SMC is actually weaker when Sahel rainfall is enhanced, and that the negative correlation between Sahel precipitation and low-level geopotential occurred primarily because of a concurrent northward shift of the precipitation maximum and the SMC. The idea that Sahel precipitation is inhibited by a stronger SMC is supported by the results of Peyrillé and Lafore (2007), who found that the effect on precipitation of the mid-level warming

and drying was stronger than that of the near-surface cooling and moistening when the two components of the vertical dipole were imposed separately in an idealized model. In separate work that did not even mention monsoons, Sobel and Bellon (2009) also found that advective drying in the middle troposphere can be highly effective at suppressing precipitation. They imposed drying tendencies at different levels of two single-column models, with these tendencies intended to represent horizontal moisture advection, and found that precipitation was more sensitive to middle-tropospheric drying than to lower-tropospheric drying. Their lower-tropospheric drying was imposed in the 825–600 hPa layer, and thus may be a better analogue for moisture advection in the upper branch of the SMC, but this nevertheless illustrates the potential for horizontal moisture advection at least a few kilometres above the surface to alter rainfall.

Although previous work has thus provided evidence for the suppression of monsoon precipitation by the horizontal advection of dry, mid-tropospheric air into the humid parts of West Africa, South Asia, and Australia, that previous work focused on a variety of time-scales in a number of isolated regions. Regional intercomparisons and global analyses of SMCs have been conducted (e.g. Trenberth *et al.*, 2000; Zhang *et al.*, 2008), but these have examined SMC winds rather than the moisture advection produced by SMCs. It remains unclear whether the intensity and vertical structure of the drying tendencies produced by SMCs is similar across all monsoon regions, and whether advection by time-mean SMC winds dominates advection by transient eddies. One goal of this study is thus to document and compare the distributions of horizontal advective drying in four monsoon regions during local summer: West Africa, South Asia, southern Africa, and Australia. All of these regions have been shown to have prominent SMCs in the local summer mean (Nie *et al.*, 2010). Here we ask, in particular, whether horizontal advective drying a few kilometres above the surface has comparable strength and vertical structure in all regions, and whether it is produced primarily by time-mean winds or by transient eddies. Furthermore, if transient eddy advection of moisture is large, can it be represented as a simple down-gradient diffusion of moisture? It seems plausible, for example, that transient eddy advection of moisture might be stronger in West Africa than in other regions because of the prominence of African easterly waves, which are known to advect momentum meridionally (e.g. Reed *et al.*, 1977; Straub *et al.*, 2006), and that it might not be possible to describe moisture transport by these waves in terms of a simple eddy diffusion. Resolution of these issues is important for constructing accurate conceptual and theoretical models of monsoons.

To be clear, we focus on horizontal rather than vertical advection in this paper because vertical motion cannot be viewed as a cause of precipitation. In contrast, horizontal flow in SMCs is controlled by boundary-layer temperature gradients tied to surface conditions, and that flow produces horizontal advection that is more widely viewed as a control on precipitating convection. To illustrate this, we briefly introduce the vertically integrated moisture budget, following Seager and Henderson (2013):

$$P - E = -\frac{1}{g} \frac{\partial}{\partial t} \int_0^{p_s} q \, dp - \frac{1}{g} \int_0^{p_s} q (\nabla \cdot \mathbf{u}) \, dp - \frac{1}{g} \int_0^{p_s} (\mathbf{u} \cdot \nabla q) \, dp - \frac{q_s}{g} \mathbf{u}_s \cdot \nabla p_s. \quad (1)$$

Here the difference between precipitation  $P$  and surface evapotranspiration  $E$  is balanced by the time rate of change of vertically integrated moisture, the convergence of horizontal wind  $\mathbf{u}$  having specific humidity  $q$ , horizontal advection of humidity, and a boundary term that involves the surface values of horizontal wind, humidity, and pressure  $p$  (with  $g$  the gravitational acceleration). Although the surface term can be locally large, its magnitude is due almost entirely to surface pressure gradients

associated with orography; scale analysis shows that dynamically generated surface gradients make a contribution to this term that is more than an order of magnitude smaller. The second term on the right-hand side, which is often large, can alternately be expressed as vertical advection of moisture and thus depends on vertical motion. But in low latitudes, vertical velocity cannot be viewed as a cause of precipitating convection; when the Coriolis parameter is small, weak horizontal temperature gradients allow vertical motion  $\omega$  to be diagnosed from the diabatic heating in a selected column of the atmosphere (Sobel *et al.*, 2001),

$$\omega \simeq \frac{Q_c}{S} \quad (2)$$

where  $Q_c$  is the convective heating and  $S$  is a static stability. The vertical integral of  $Q_c$  is equal to  $P$  on the left-hand side of (1) so, under the weak temperature gradient approximation, the vertical advective term in the moisture budget becomes a function of the precipitation itself and thus cannot be viewed as a control on precipitation. Vertical motion and precipitation are strongly correlated in the Tropics, and neither can be viewed as causing the other (e.g. Emanuel *et al.*, 1994). In contrast, horizontal flow in SMCs is associated with horizontal boundary-layer temperature gradients between deserts and adjacent vegetated or ocean regions, and cannot be inferred from vertical motion in the deep, precipitating component of the circulation. For example, 700 hPa horizontal flow in the Saharan SMC consists partly of geostrophic flow in the anticyclone above the desert heat low, and partly of the ageostrophic overturning circulation in that heat low; neither of these components can be obtained given the precipitation. This is why numerical studies of precipitation in a single atmospheric column have imposed mid-tropospheric drying as an idealized proxy for horizontal moisture advection (e.g. Sobel and Bellon, 2009), and why observational studies view horizontal moisture advection as a control on precipitation (e.g. Parker *et al.*, 2016).

The next section of this paper describes the data used in this study. The time-mean structure of SMCs over different continents are then presented in section 3, followed by analyses of horizontal advective drying in section 4. We summarize and discuss implications in section 5.

## 2. Data sources and analysis procedure

We used six-hourly data for 1979–2014 from ERA-Interim, the latest global atmospheric reanalysis from the European Centre for Medium-Range Weather Forecasts. We used data that were regridded to a resolution of approximately  $0.7^\circ \times 0.7^\circ$  in the horizontal with 37 pressure levels. We compared the summer mean vertical structure of meridional wind in ERA-Interim with that obtained from *in situ* measurements from the Atmospheric Radiation Measurement (ARM) Program (<http://www.arm.gov>; accessed 24 June 2017) of the US Department of Energy. The ARM measurements include Vaisala-processed horizontal winds every 6 h from the balloon-borne sounding system at Darwin, Australia ( $12^\circ\text{S}$ ,  $131^\circ\text{E}$ ) for 2002–2009.

For precipitation, we used estimates from the Tropical Rainfall Measuring Mission (TRMM) product 3B42 for 1998 to 2012, which provides 3-hourly precipitation rates at a horizontal resolution of  $0.25^\circ \times 0.25^\circ$ . When examining interannual variability, we also employed monthly averaged precipitation data from the Global Precipitation Climatology Project (GPCP) at  $2.5^\circ$  horizontal resolution from 1979 to 2015.

Summer means were calculated over June–August for Northern Hemisphere monsoon regions and December–February for Southern Hemisphere regions, and all results presented here are climatologies averaged over all years of the relevant dataset. Horizontal moisture advection by the total flow was directly computed using six-hourly ERA-Interim data, then these horizontal advective tendencies were averaged over the local summer periods of all 36 years in our ERA-Interim sample. The advection of moisture

by transient eddies was calculated by subtracting the horizontal advective tendency produced by the time-mean flow (i.e. the climatological summer mean horizontal flow acting on the climatological mean specific humidity distribution) from the total horizontal advection.

## 3. Regional climatologies of shallow monsoon flow

We begin by briefly examining the climatological mean horizontal and vertical structure of SMCs in four monsoon regions during local summer. Although some properties of SMCs have been compared across different regions, these intercomparisons have focused more on the cross-equatorial flow rather than that in the off-equatorial monsoon precipitation maxima (e.g. Zhang *et al.*, 2008). No intercomparison of the horizontal and vertical structures of these circulations and their relation with the distributions of humidity and monsoon precipitation has been published.

The summer-mean circulation in monsoon regions typically includes an anticyclone centred several kilometres above the surface, around 700 hPa (Figures 1(a), (c) and (d)). The lower-latitude part of each anticyclone constitutes the upper branch of the local SMC, in which equatorward flow is directed across strong horizontal gradients of relative humidity into the region of high precipitation (which is outlined in cyan in Figure 1). These anticyclones are approximately in geostrophic balance: the scales of the Australian anticyclone, for example, yield a Rossby number less than 0.1.

Substantial regional differences exist in the horizontal structure and magnitude of flow in these SMCs. Equatorward flow in the upper branch of an SMC is strongest and most horizontally extensive in West Africa, where northeasterly winds with magnitude around  $10 \text{ m s}^{-1}$  stretch thousands of kilometres across the entire Sahel at 700 hPa (Figure 1(a)). The horizontal structure of the 700 hPa anticyclone is highly asymmetric over West Africa, with southward flow on its eastern side much more zonally confined than northward flow on its western side. The anticyclones over southern Africa and Australia are more symmetric and have equatorward flow into the monsoon precipitation maximum that is weaker than that seen over West Africa (Figures 1(c) and (d); we show fields at 600 hPa for southern Africa because orography in that region seems to shift the SMC there to lower pressures, a phenomenon shown in more detail below). Flow in the higher-latitude halves of the Australian and southern African anticyclones has merged with the midlatitude westerlies, and it is primarily the eastern branch of these two anticyclones that is directed along a strong dry-to-moist horizontal gradient in relative humidity. In contrast, it is the southern part of the West African anticyclone that crosses contours of relative humidity. The summer-mean humidity field over southern Africa seems to be highly distorted by the anticyclone, with a tongue of dry air wrapping around that anticyclone's centre into the eastern side of the precipitating region. We expect horizontal advection to alter the humidity field in all regions; deformation of humidity contours consistent with that hypothesis is also seen over Australia, and the moist region at 700 hPa is likely shifted southward over West Africa and southeastward over South Asia by the shallow flow.

The 700 hPa flow in South Asia is distinct from that in other regions, presumably because lower-tropospheric horizontal flow there is highly modified by orography. During boreal summer, strong low-level monsoon westerlies extend across the entire South Asian region between the Equator and  $15^\circ\text{N}$ , and substantial precipitation falls over much of the Indian Ocean and continental India (Figure 1(b)). The SMC is evident as northerly and northwesterly flow at 700 hPa across Pakistan, the northern Arabian Sea, and the northern two-thirds of India. This is outflow from the intense desert heat low centred over Pakistan and northwestern India (Bollasina *et al.*, 2011), which has been shown to dry the lower and middle troposphere over continental

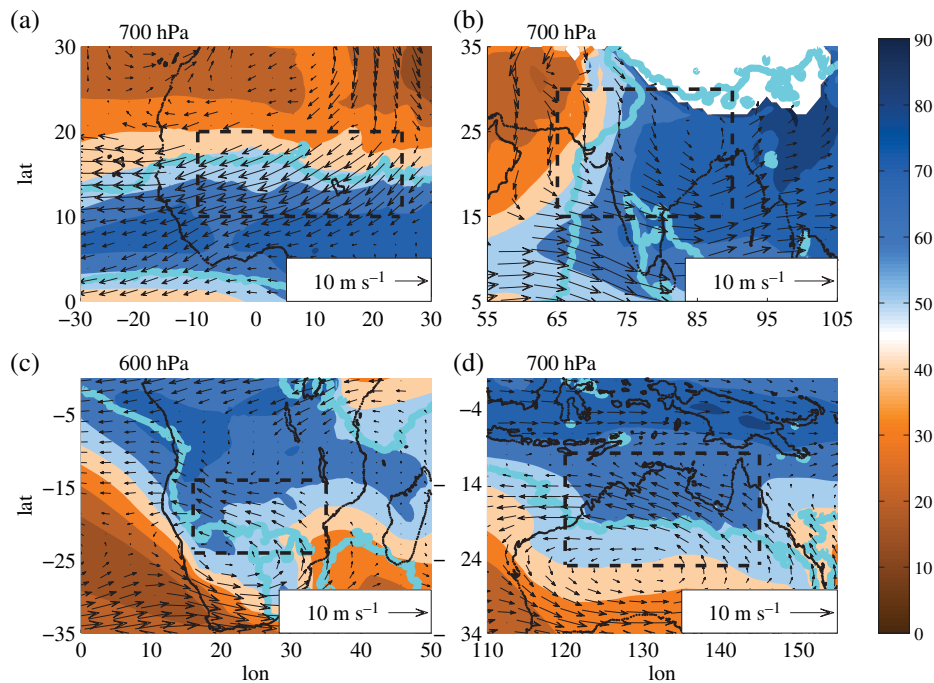


**Figure 1.** Relative humidity (RH, %, shading) and horizontal velocity ( $\text{m s}^{-1}$ , vectors) averaged June–August for (a) West Africa and (b) South Asia, and averaged December–January for (c) southern Africa and (d) Australia, at 600 hPa in (c) and at 700 hPa in (a, b, d). The cyan line surrounds regions where the precipitation is larger than 2, 4, 3, and 4  $\text{mm day}^{-1}$  in (a), (b), (c) and (d), respectively. The dashed rectangular boxes mark regions over which horizontal means are shown in later figures. [Colour figure can be viewed at [wileyonlinelibrary.com](http://wileyonlinelibrary.com)].

India, particularly during early summer (Parker *et al.*, 2016). A clear contrast with the other regions is that the humidity gradient in South Asia is primarily zonal, so that it is likely the zonal component of the shallow flow that accomplishes most of the moisture advection there. The South Asian monsoon thus lacks a clear 700 hPa anticyclone positioned over a desert heat low. Nevertheless, time-mean southeastward flow from the deserts of southwestern Asia clearly advects dry air into the monsoon region.

We now examine the vertical structure of shallow flow in each region by horizontally averaging meridional wind over land within boxes that demarcate the four monsoon regions. West African winds are averaged from 10 to 20°N and 10°W to 25°E, which is similar to definitions of the Sahel used in previous studies (e.g. Janowiak, 1988; Biasutti and Sobel, 2009; Giannini *et al.*, 2013). South Asian winds are averaged from 15 to 30°N and 65 to 90°E, a region that excludes the southern tip of India but includes nearly all of the rest of India, and parts of Nepal and Bangladesh. Winds in southern Africa were averaged from 16 to 35°E and from 14 to 24°S; although southern Africa is sometimes not regarded as a major monsoon region, it is home to a seasonal precipitation maximum that exhibits many of the dynamical features of monsoons (McHugh, 2004; Nie *et al.*, 2010; Hurley and Boos, 2013). Australian winds are averaged from 10 to 25°S and 120 to 145°E, an area that includes the ‘top end’ rainfall that constitutes the Australian monsoon (Wheeler and McBride, 2005; Wang and Ding, 2008; Colman *et al.*, 2011). Our exact choice of boundaries in each region was guided by the desire to include regions with equatorward flow in the lower mid-troposphere, ensuring that our regional averages characterize the local SMC. Averages were taken only over land within each of these boxes in order to make our results relevant to continental precipitation, but including ocean regions yielded qualitatively similar results.

Comparison of the regionally averaged wind shows that the vertical structure of meridional flow in SMCs is highly similar across all four monsoon areas (Figure 2(a); the sign of meridional wind has been chosen so that poleward flow is positive). Low-level poleward flow in all regions is confined within 150 hPa of the Earth’s surface, and the upper branch of the SMC is evident as equatorward flow that peaks between 600 and 700 hPa (note that the upper-tropospheric wind does not show clear evidence of a monsoonal meridional overturning, for reasons discussed in the

next paragraph). The transition from poleward to equatorward flow occurs at about 850 hPa in all regions except southern Africa. Our southern Africa region has a mean surface pressure around 900 hPa, and this reduced surface pressure is associated with a lifting of the entire vertical structure of the SMC. The upper branch of the SMC is strongest in West Africa and weakest over southern Africa. In contrast to the similarities seen in the profiles of meridional flow, the vertical structures of zonal velocity have large regional differences (Figure 2(b)). Near-surface monsoon westerlies are seen only in the regional averages for West Africa and South Asia, because the near-surface monsoon westerlies in Australia and southern Africa are weaker and confined to the equatorial edge of the averaging domain for those regions. As mentioned above, the 700 hPa zonal wind is easterly in all regions except South Asia, where the flow is strongly influenced by orography and the desert outflow is directed to the southeast across continental India.

Above the SMC, the vertical structure of the meridional wind has large regional differences. Upper-tropospheric flow over West Africa is poleward because the Sahel lies north of the African monsoon precipitation maximum; Sahelian upper-level flow is thus characteristic of the summer cell of the solstitial Hadley circulation. In contrast, our Australian and South Asian averages are dominated by the regional upper-tropospheric anticyclones. Northern Australia lies slightly closer to the eastern branch of that upper-tropospheric anticyclone (not shown) and thus exhibits equatorward flow at 200 hPa, while India lies closer to the western part of the upper-tropospheric anticyclone and so has poleward 200 hPa flow. Figure 2(a) shows that the low-level poleward flow is weaker and occurs over a much thinner pressure layer than the equatorward flow in the upper branch of the SMC, suggesting an imbalance between the poleward and equatorward mass fluxes, but this is partly an artifact of only plotting values at pressures lower than the time-mean, regional-mean surface pressure (although the meridional flow need not vertically integrate to zero since it is averaged over a limited range of longitudes). For instance, in South Asia near-surface poleward flow is directed through the eastern and western ends of the Indo-Gangetic plain, near sea level in a region where the mean surface elevation is substantially higher (e.g. Boos and Hurley, 2013, their Figure 3). Since the main focus of this paper is the advective

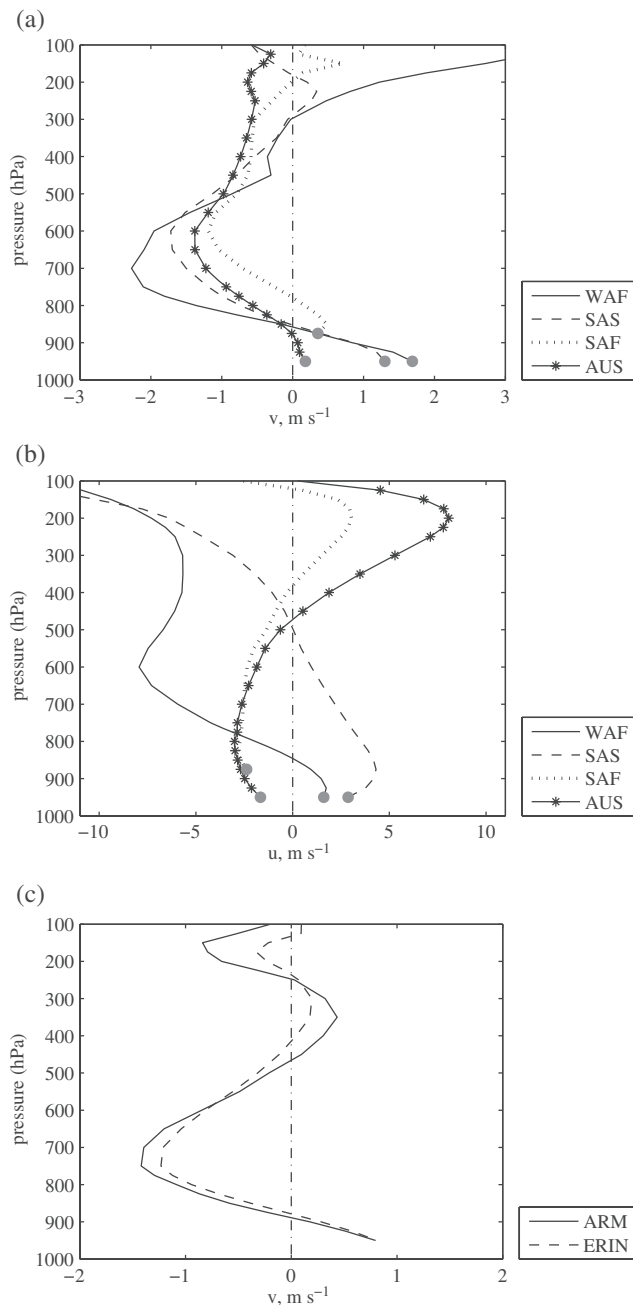


**Figure 2.** Vertical profiles of (a) meridional velocity and (b) zonal velocity during local summer over West Africa (solid), South Asia (dashed), southern Africa (dotted) and Australia (asteroid), averaged over land regions within the boxes shown in Figure 1. Negative values indicate equatorward flow and positive indicate poleward flow. (c) shows the climatological vertical structure of meridional velocity over Darwin, Australia from ARM *in situ* measurements at Darwin from 2002 to 2009 (solid) and from ERA-Interim reanalysis product at the grid point nearest Darwin (12.5°S, 130.8°E). Data below the time- and horizontal-mean surface pressure level (which is marked by the grey circles) are not presented.

drying in the upper branch of the SMC, we do not attempt to accurately diagnose the time-mean near-surface poleward mass flux in each region.

We recognize that all of this discussion has focused on reanalyzed winds which may be poorly constrained by direct observations in many of the regions studied here. For this reason, we compare the vertical structure of meridional wind from ERA-Interim with that obtained from radiosondes in Darwin, Australia. The time-mean ERA-Interim meridional wind compares quantitatively well with these *in situ* measurements, showing near-surface poleward flow and strong return flow in the upper branch of the SMC (Figure 2(c)).

In summary, all four monsoon regions contain time-mean shallow circulations, with the West African circulation being the strongest and the southern African circulation the weakest. The

upper part of these shallow circulations consists of an anticyclone centred near 700 hPa, except in South Asia where the horizontal structure of the flow is highly distorted by orography. The vertical structure of the regionally averaged meridional mass flux is highly similar across all regions, with the equatorward mass flux in the upper branch of the SMCs peaking at 600–700 hPa and spanning a layer of the middle troposphere that is roughly 500 hPa thick. However, only in West Africa does the SMC outflow seem to consist of strongly divergent flow that passes through the monsoon precipitation maximum. The upper branch of the SMC in Australia and southern Africa seems to be more rotational and does not penetrate the deep ascent zone, deviating from the schematic shown in Nie *et al.* (2010), their Figure 6b. Still, in all regions the structure of the wind and humidity fields at 700 hPa suggests that these time-mean shallow circulations advect mid-tropospheric dry air into the precipitating monsoon zone (e.g. Figure 1); this moisture advection is examined in more detail in the next section.

#### 4. Drying tendency of shallow flow

To begin our study of the mid-level drying produced by SMCs, we first examine the vertical distribution of horizontal moisture advection averaged over each of the continental regions described above. As expected, these vertical profiles of total horizontal moisture advection show a general pattern of near-surface moistening and mid-level drying (Figure 3). The peak advective moistening occurs near the surface while the peak drying lies between 750 and 800 hPa. The peak drying occurs at lower altitudes than the peak equatorward wind (compare with Figure 2) because the scale height of water vapour, roughly 2 km, is smaller than the depth of the SMC. The peak mid-level drying is of similar magnitude across all regions, peaking between 0.5 and 1 g kg<sup>-1</sup> day<sup>-1</sup>. The vertical profile for West Africa agrees with that computed by Peyrillé and Lafore (2007).

The relative contribution of time-mean flow and transient eddies to the total moisture advection varies greatly between regions. Advection of time-mean humidity by time-mean winds accounts for most of the total horizontal advection in both of our Northern Hemisphere monsoon regions, while advection by transient eddies is more important in the Southern Hemisphere regions (compare dashed and solid lines in Figure 3). Transient eddy advection is particularly strong over northern continental Australia, where it accounts for at least 80% of the peak total horizontal advection. This disproves the idea that advective drying by transient eddies will be strongest over West Africa because of the prominence of African Easterly Waves. Although oceanic regions were excluded from the horizontal averages for South Asia and Australia, including those oceanic regions does not qualitatively change the vertical profiles of total or eddy drying tendencies (not shown).

Additional insight can be gained by examining the horizontal distribution of horizontal moisture advection, and we do so on the pressure level at which the maximum drying tendency occurs (800 hPa for South Asia, 775 hPa for Australia, and 750 hPa for West Africa and southern Africa). The advective drying has strong horizontal inhomogeneity in South Asia, where the west coast of India shows particularly intense drying by horizontal advection. This is one region where the idea that horizontal advective drying can be viewed as a forcing for precipitation breaks down, because much precipitation in this region is forced by large-scale ascent over the orography of the Western Ghats; horizontal and vertical advection of moisture will strongly cancel each other when large-scale flow ascends along those mountain slopes. However, over the rest of non-peninsular India, the horizontal advective drying is more uniform in the horizontal and can be attributed to the dry, northwesterly flow discussed by Parker *et al.* (2016). South Asia is also the only region that exhibits strong drying by horizontal advection over large parts of the ocean, particularly over the eastern Arabian Sea. That unique feature exists because strong westerly outflow from the Somali jet is superimposed on a

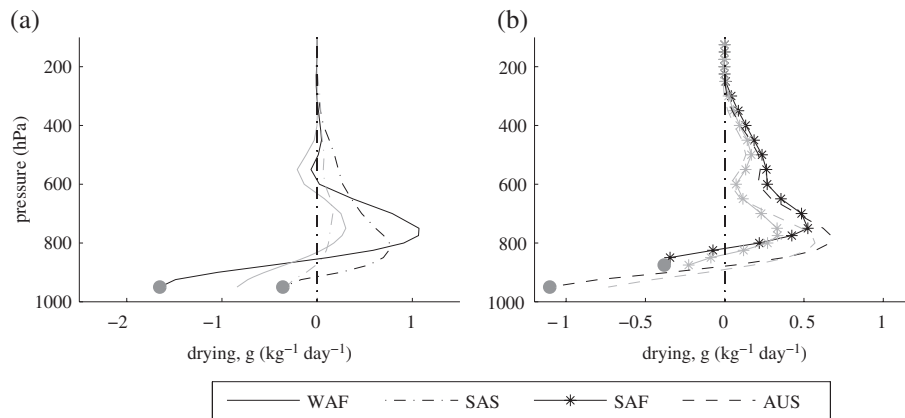


**Figure 3.** Vertical profiles of horizontal moisture advection,  $\overline{\mathbf{u} \cdot \nabla q}$ , averaged during local summers and over land in the boxes indicated in Figure 1. Units are  $\text{g kg}^{-1} \text{ day}^{-1}$  and colours denote the same regions as in Figure 2. The sign is chosen so that a positive number denotes a drying tendency. Black lines show the tendency produced by the total flow and gray lines show the tendency produced by transient eddies. Grey circles mark the time- and horizontal-mean surface pressure.

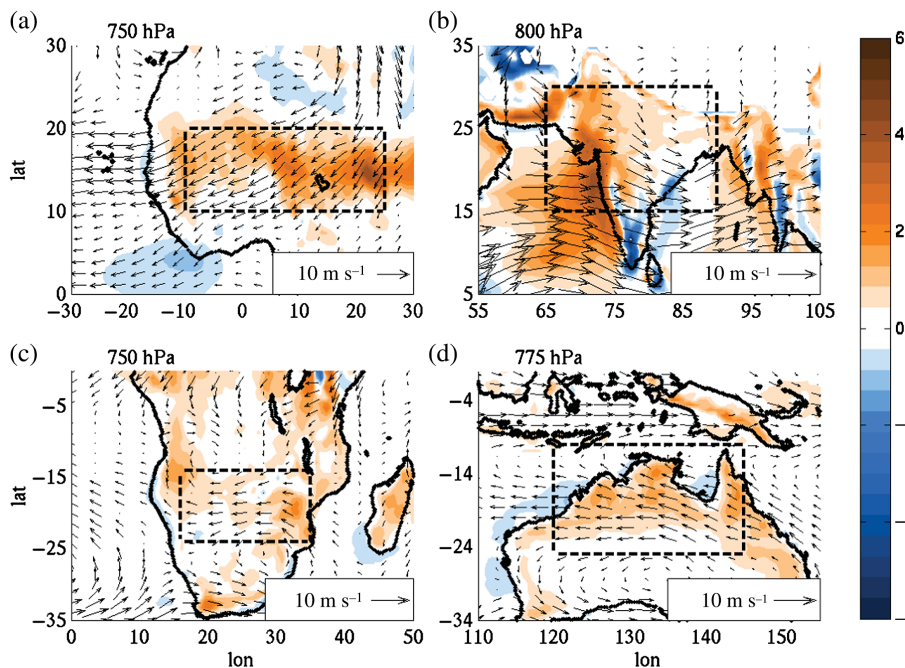


**Figure 4.** Drying tendency ( $\overline{\mathbf{u} \cdot \nabla q}$ ,  $\text{g kg}^{-1} \text{ day}^{-1}$ , shading) and horizontal wind ( $\text{m s}^{-1}$ , vectors) averaged during local summer. In each region these quantities are plotted at the level at which the regionally averaged drying tendency (shown in Figure 3) is a maximum: (a) 750 hPa, (b) 800 hPa, (c) 750 hPa and (d) 775 hPa for West Africa, South Asia, southern Africa and Australia, respectively. The contour interval for the shading is  $0.4 \text{ g kg}^{-1} \text{ day}^{-1}$ . [Colour figure can be viewed at [wileyonlinelibrary.com](http://wileyonlinelibrary.com)].

strong zonal humidity gradient (Figure 2(b)). In all other regions the horizontal advection around 800 hPa produces drying over continents and weaker moistening over ocean, often with a sharp boundary between the two at the coast.

Since transient eddies produce a large fraction of the total horizontal moisture advection in some regions, we wish to better understand the distribution and general nature of this eddy advection. As expected from the regionally averaged vertical profiles of advection discussed above, the horizontal distribution of advective drying by transient eddies is similar to that of the total horizontal advection in southern Africa and in Australia (compare (c) and (d) of Figures 5 and 4, noting the change in colour scale). This similarity is particularly strong in Australia; in southern Africa the eddy drying is strongest over the western part of our continental box while the total advective drying is strongest in the eastern part of that box. Eddy drying is weak over India and West Africa, although eddy moistening is strong over the southwestern coast of India. However, the drying by the mean flow (the total minus the eddy drying) has an even stronger drying effect over the western coast.

One common way to represent the horizontal advection produced by transient eddies is via an ‘eddy diffusion’ that acts on the

time-mean quantity being advected. In an idealized model, Sobel and Neelin (2006) showed that the intensity and meridional width of the intertropical convergence zone (ITCZ) could be controlled by changing the horizontal eddy diffusion of moisture. In this spirit, we calculated the two-dimensional Laplacian of specific humidity on the same pressure levels used for plotting the horizontal distributions of transient eddy advection, and multiplied this by a constant diffusivity of  $5 \times 10^5 \text{ m}^2 \text{ s}^{-1}$ . This diffusivity was chosen subjectively to roughly match the observed magnitude of the transient eddy advective drying, but it lies in the range of values used in idealized models for tropical dynamics (e.g. Neelin and Zeng, 2000; Sobel and Neelin, 2006). Since the second derivatives in the Laplacian produce high variance at fairly short spatial scales, we introduced a weak smoothing by applying a 1-2-1 filter one time each in latitude and longitude. Additional smoothing could be obtained by successive application of this filter.

Our parametrized eddy diffusion matches the transient eddy advection most closely in the Southern Hemisphere (Figure 6; a contour of eddy diffusion is superimposed on the transient eddy advection in Figure 5 to ease comparison). Although most features in the spatial distribution of the eddy diffusion are too sharp, the diffusive drying otherwise matches the eddy advective

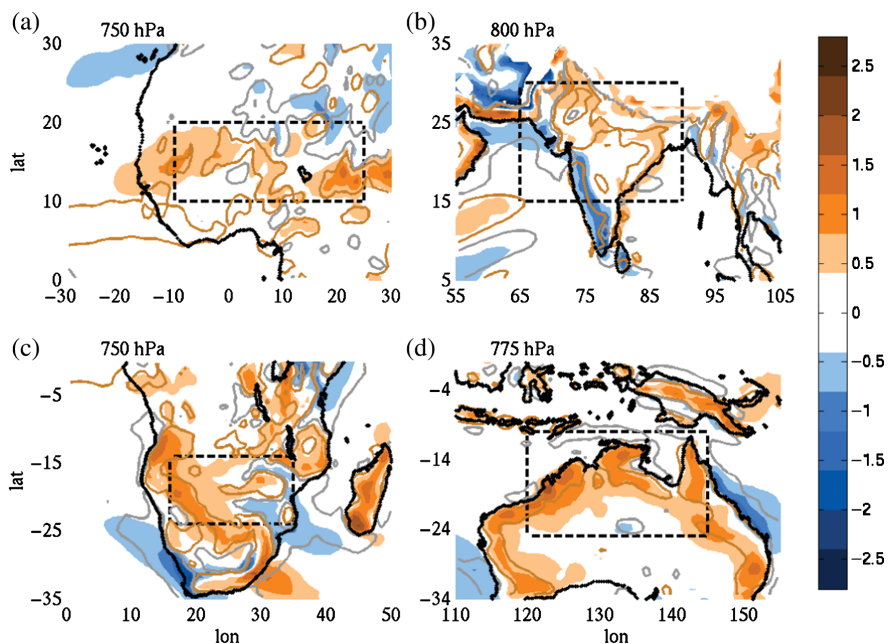


**Figure 5.** Drying tendency by transient eddies ( $\overline{\mathbf{u}' \cdot \nabla q'}$ ,  $\text{g kg}^{-1} \text{ day}^{-1}$ , shading), averaged during local summer at the same levels as in Figure 4. The contour interval is  $0.4 \text{ g kg}^{-1} \text{ day}^{-1}$ , as in Figure 4, but note the smaller range used for the colour scale. Solid contours outline regions where our eddy moisture diffusion (see text for details) has a magnitude larger than  $0.4 \text{ g kg}^{-1} \text{ day}^{-1}$ , with the orange contour signifying diffusive drying and the grey diffusive moistening. [Colour figure can be viewed at [wileyonlinelibrary.com](http://wileyonlinelibrary.com)].

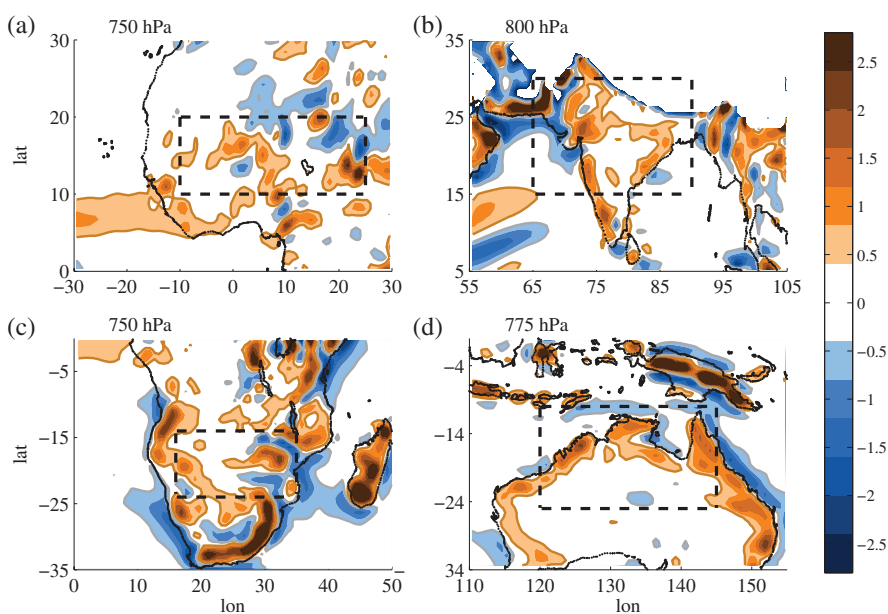


**Figure 6.** Our parameterized eddy diffusion of moisture, represented as the horizontal Laplacian of specific humidity with a diffusivity of  $5 \times 10^5 \text{ m}^2 \text{ s}^{-1}$ , at the same levels as in Figure 4. Orange shading denotes drying and blue moistening, plotted with an interval of  $0.4 \text{ g kg}^{-1} \text{ day}^{-1}$ . Orange and grey contours denote  $\pm 0.4 \text{ g kg}^{-1} \text{ day}^{-1}$ , respectively. Modest smoothing was achieved by applying a 1-2-1 filter in latitude and longitude. [Colour figure can be viewed at [wileyonlinelibrary.com](http://wileyonlinelibrary.com)].

drying well over the coastal regions of Australia, southern Africa, Madagascar, and Indonesia/Papua New Guinea. The agreement is poorer over South Asia and West Africa. One particularly notable disagreement is in the Atlantic ITCZ, where the diffusive estimate predicts drying of about  $0.5 \text{ g kg}^{-1} \text{ day}^{-1}$  while the transient eddy advection is close to zero and the total horizontal moisture advection produces moistening in the eastern part of that region (compare (a) in Figures 4–6). Weak moisture advection in the eastern Atlantic ITCZ by the time-mean horizontal wind is expected because the time-mean wind is directed parallel to that ITCZ; the mid-tropospheric Saharan anticyclone produces only weak southward flow as far south as that ITCZ region, and the eddy moisture advection produced by African Easterly Waves seems to be weak there.

To the degree that transient eddy advection can be represented by a diffusive approximation over continental Australia and

southern Africa, eddy drying should not be thought of as being large only in regions where there is a local humidity maximum. That is, eddy diffusion is large where the curvature of the humidity field (i.e. the two-dimensional Laplacian) is large, and large curvature often occurs in regions far from humidity maxima (we do not show the time-mean specific humidity field because it looks very much like the relative humidity field shown in Figure 1). For example, diffusive drying is strong over coastal Australia, but one would have a difficult time identifying a region of strong curvature there by eye. In contrast, the humidity field has a local maximum over Papua New Guinea (Figure 1(d)), which produces strong diffusive drying there (Figure 6(d)). Although these distributions of diffusive drying are a straightforward consequence of the approximation of the diffusive flux as being proportional to the humidity gradient, they provide a useful reminder that transient eddy drying need not occur in only the

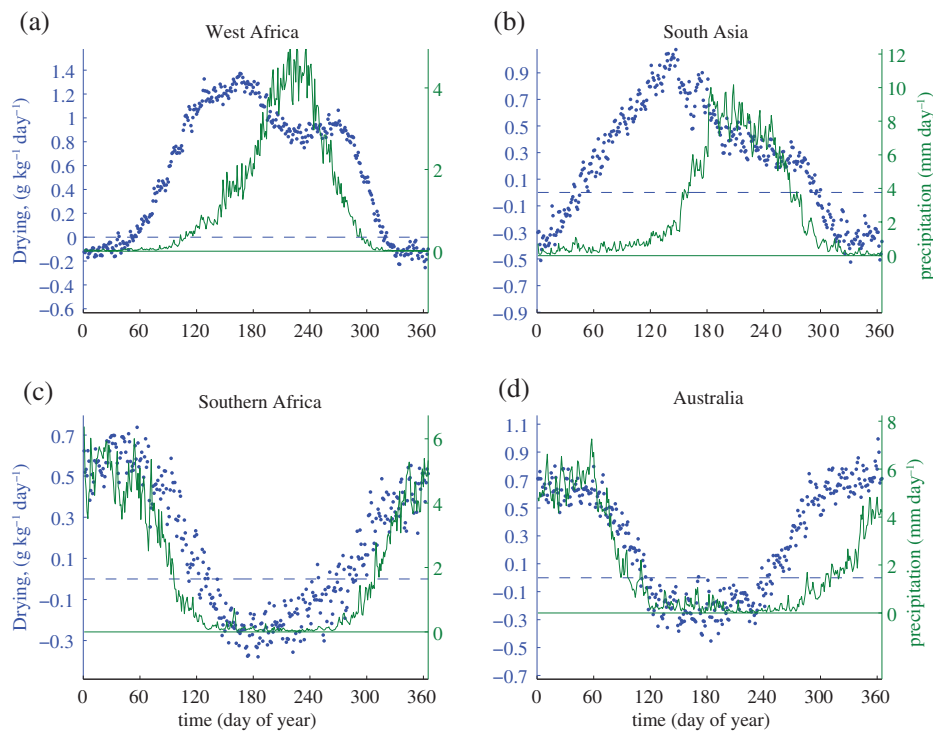


**Figure 7.** Daily climatologies of the horizontal advective drying tendency ( $\text{g kg}^{-1} \text{day}^{-1}$ , dotted) and of precipitation ( $\text{mm day}^{-1}$ , solid), horizontally averaged over land in the boxes shown in Figure 1. The horizontal advective drying is from the same levels shown in Figures 4–6, where the summer mean, regionally averaged, drying peaks. Horizontal dashed lines mark zero for advective drying (dashed) and precipitation (solid). [Colour figure can be viewed at [wileyonlinelibrary.com](http://wileyonlinelibrary.com)].

most humid regions. Generally, much of the fine-scale structure in the transient eddy drying can be accounted for by eddy diffusion; the fine-scale structure shown in Figure 5 can thus be largely understood as arising from the curvature of the humidity field. This curvature, in turn, is likely shaped by circulations such as coastal sea breezes, orographically modified winds, and the time-mean SMCs.

What consequence might these distributions of advective drying have for monsoon precipitation? In an idealized model of a single column of the atmosphere, Sobel and Bellon (2009) found that a drying tendency of  $1 \text{ g kg}^{-1} \text{day}^{-1}$  in the 600–825 hPa layer produced a rainfall reduction of about  $10 \text{ mm day}^{-1}$ . Thus, the advective drying shown in Figure 4 would seem to be sufficiently large to produce strong reduction in rainfall. The effect of this mid-tropospheric drying would be opposed by that of the near-surface moistening, and horizontal temperature advection will also influence precipitation. As mentioned in the Introduction, Peyrillé and Lafore (2007) found that the negative effect of mid-level warming and drying on an idealized simulation of Sahel rainfall was stronger than the positive effect of near-surface cooling and moistening. But they showed results only for 20 simulated days in one zonally symmetric model, so further investigation seems warranted.

The seasonal cycles of precipitation and mid-tropospheric drying tendency in West Africa and South Asia are consistent with the hypothesis that advective drying inhibits precipitation (Figure 7, which shows regionally averaged precipitation and horizontal advective drying tendency at the levels at which the regionally averaged, summer mean drying tendency peaks). In West Africa the advective drying at 750 hPa peaks in June (near calendar day 160), then decreases as summer progresses and the precipitation rate increases. This advective drying over the Sahel is about two-thirds as strong in August–September as it is in June. Zhang *et al.* (2008) suggested that the West African SMC might inhibit the northward migration of precipitation over the Sahel during early summer by advecting ‘dry, warm, and perhaps dusty, air from the heat low into the monsoon rainband’ (also Parker *et al.*, 2005), but to our knowledge no previous studies have documented the seasonal cycle of advective drying in that region. Advective drying in South Asia is also stronger prior to

the onset of summer rainfall. Its gradual summer decrease in our South Asian box would be consistent with the finding of Parker *et al.* (2016) that precipitation spreads to the northwest over India while the advective drying contracts to the northwest. In contrast, there is no clearly discernable decrease in advective drying that accompanies the onset of summer rainfall in Australia and southern Africa. In those regions advective drying increases in spring (from day 250–300), and does not decrease when summer precipitation starts around day 320.

In future work, we hope to use multiple observational datasets to investigate the influence of SMCs on the seasonal evolution of the vertical structure of moisture in these continental regions. Preliminary results (not shown) suggest that, in all regions, the seasonal cycle of precipitable water is approximately in phase with the seasonal cycle in precipitation, but the increase of precipitable water in spring and early summer is more gradual than that of precipitation. This would be consistent with previous oceanic observations of a rapid increase of precipitation at large values of precipitable water (e.g. Bretherton *et al.*, 2004). Furthermore, the seasonal cycle of mid-tropospheric dry advection seems to be more closely associated with the seasonal cycle in SMC strength rather than in moisture gradients (also not shown), highlighting the potential importance of the dry dynamics of SMCs for the seasonal evolution of monsoon precipitation.

Finally, we examine interannual variations in the seasonal mean strength of the advective drying by regressing the regionally averaged horizontal advective drying onto the linearly detrended, regionally averaged precipitation. As in our previous analyses, we use the horizontal advective drying at the pressure level at which the summer mean, regionally averaged advective drying peaks. Three of our four regions exhibit a negative correlation between this advective drying and summer precipitation which is highly significant (Figure 8). The linear regression coefficients over southern Africa, Australia, and West Africa range from roughly  $-0.1$  to  $-0.3 \text{ g kg}^{-1} \text{day}^{-1} / (\text{mm day}^{-1})$ , which is roughly consistent with our aforementioned estimate that a horizontal advective drying tendency of  $1 \text{ g kg}^{-1} \text{day}^{-1}$  reduced rainfall by  $10 \text{ mm day}^{-1}$  in an idealized model (Sobel and Bellon, 2009); here we regressed advective drying on precipitation, rather than the

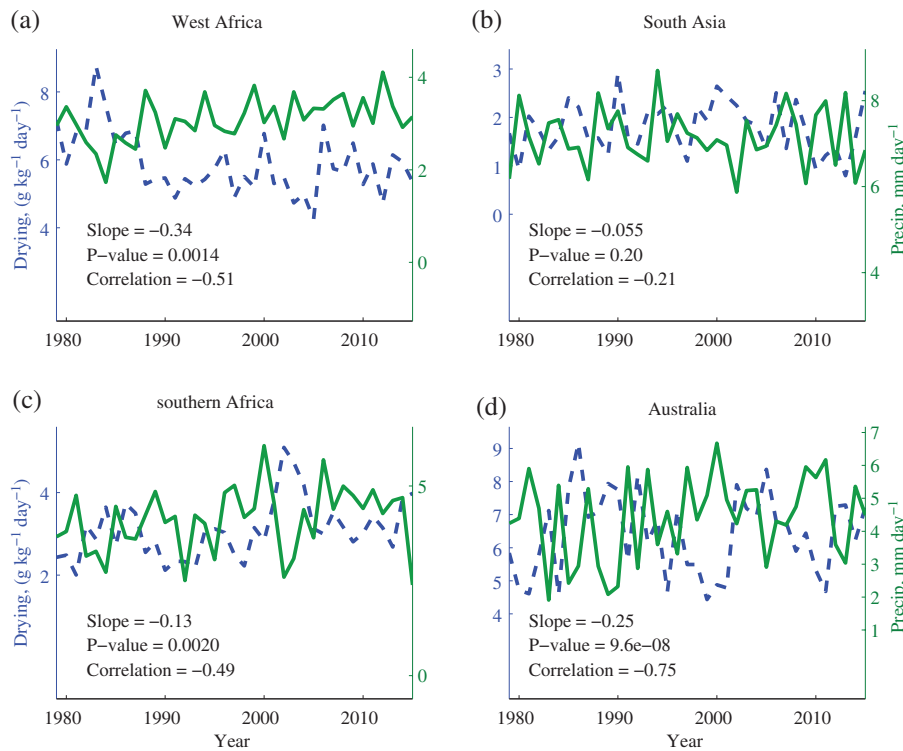


**Figure 8.** Seasonal averages of the horizontal advective drying tendency ( $\text{g kg}^{-1} \text{day}^{-1}$ , dashed) and precipitation ( $\text{mm day}^{-1}$ , solid), horizontally averaged over land in the boxes indicated in Figure 1. The horizontal advective drying is from the same levels shown in Figures 4–7, where the summer mean, regionally averaged, drying peaks. The time series plotted are not detrended, but the statistical summary of the interannual variability for each region shown in each panel is calculated from the time series with the trends removed. [Colour figure can be viewed at [wileyonlinelibrary.com](http://wileyonlinelibrary.com)].

reverse, because we expect the errors in advective drying to be larger than those in precipitation. The regression relationship over South Asia is not statistically distinct from zero. Nevertheless, this analysis of interannual variability is consistent with the hypothesis that horizontal advective drying in the outflow layer of SMCs inhibits seasonal mean monsoon precipitation.

## 5. Summary and discussion

Here we documented the climatological summer mean structure of SMCs in the monsoon regions of West Africa, South Asia, southern Africa, and Australia, then compared the horizontal advective drying tendency produced by time-mean flow in those SMCs with that produced by transient eddies. Regionally averaged equatorward flow in the lower mid-troposphere is strongest over West Africa and weakest in southern Africa, as is the advective drying tendency. Equatorward flow in the SMC peaks near 600–700 hPa in all regions, while the maximum drying tendency peaks between 750 and 800 hPa. The time-mean flow produces most of the summer mean horizontal moisture advection in West Africa and South Asia, while drying by transient eddies dominates in Australia and southern Africa. Although transient eddies are especially well-known in West Africa (i.e. African Easterly Waves), the advective drying produced by transient eddies is stronger over Australia and southern Africa, where this eddy drying can be well-represented as a simple harmonic diffusion with a diffusivity around  $5 \times 10^5 \text{ m}^2 \text{ s}^{-1}$ . This result is important for our understanding of monsoons because it means that horizontal moisture advection can be accounted for by knowing the time-mean flow and the time-mean humidity distribution. Existing theoretical models of monsoons (e.g. Emanuel, 1995; Neelin and Zeng, 2000; Boos and Emanuel, 2008) contain only a barotropic and first-baroclinic mode, and detailed knowledge of the vertical structure of SMCs and their influence on the moisture field is needed to construct models with additional vertical degrees-of-freedom.

We hope that future work will explore how the strength and vertical structure of SMCs are related to gradients in surface

pressure, boundary-layer temperature, and surface sensible and latent heat fluxes. Perhaps even more important is the detailed examination of the sensitivity of monsoon precipitation to near-surface cooling and moistening combined with elevated warming and drying. Our finding that summer monsoon rainfall is smaller during years when the horizontal advective drying is larger in the lower free troposphere is consistent with the hypothesis that the advective drying inhibits monsoon rainfall, but this observational analysis does not demonstrate causation. Recent work has compiled linear sensitivities of moist convection to isolated temperature and humidity tendencies using cloud-system-resolving models integrated with oceanic lower-boundary conditions (Kuang, 2010; Tulich and Mapes, 2010); application of those linear frameworks to the monsoon systems examined here may help in understanding the seasonal evolution and interannual variability of monsoon rainfall. More fundamentally, we would like to know whether the influence of horizontal moisture advection alters continental monsoon precipitation in the same way that it does oceanic precipitation, and whether the sensitivity is fundamentally altered by dynamical feedbacks with the large-scale monsoon flow.

In addition, SMCs may also affect monsoon rainfall through the advection of desert dust aerosol. For example, Jin *et al.* (2014) argued that Middle Eastern dust enhances the low-level thermal contrast in and the seasonal mean strength of the Indian monsoon. Dust aerosol has also been argued to affect monsoon rainfall on intraseasonal to interannual time-scales in India (Lau, 2014; Vиноj *et al.*, 2014; Lau *et al.*, 2016) and Africa (Yoshioka *et al.*, 2007; Zhao *et al.*, 2011). A comparison of the influence of SMC advection of heat, humidity, and dust on monsoon rainfall will thus be important for achieving a more complete understanding of monsoon dynamics.

## Acknowledgements

Both authors acknowledge support from National Science Foundation grant AGS-1253222. This work was also supported in part by the Yale Center for Research Computing.

## References

- Austin JM, Fleisher A. 1948. A thermodynamic analysis of cumulus convection. *J. Meteorol.* **5**: 240–243.
- Biasutti M, Sobel AH. 2009. Delayed Sahel rainfall and global seasonal cycle in a warmer climate. *Geophys. Res. Lett.* **36**(23).
- Biasutti M, Sobel AH, Camargo SJ. 2009. The role of the Sahara low in summertime Sahel rainfall variability and change in the CMIP3 models. *J. Clim.* **22**: 5755–5771.
- Bollasina MA, Ming Y, Ramaswamy V. 2011. Anthropogenic aerosols and the weakening of the South Asian summer monsoon. *Science* **334**: 502–505.
- Boos WR. 2015. 'A review of recent progress on Tibet's role in the South Asian monsoon'. *CLIVAR Exch.* **19**: 23–27.
- Boos WR, Emanuel KA. 2008. Wind–evaporation feedback and abrupt seasonal transitions of weak, axisymmetric Hadley circulations. *J. Atmos. Sci.* **65**: 2194–2214.
- Boos WR, Hurley JV. 2013. Thermodynamic bias in the multimodel mean boreal summer monsoon. *J. Clim.* **26**: 2279–2287.
- Boos WR, Kuang Z. 2010. Dominant control of the South Asian monsoon by orographic insulation versus plateau heating. *Nature* **463**: 218–222.
- Bretherton CS, Peters ME, Back LE. 2004. Relationships between water vapor path and precipitation over the tropical oceans. *J. Clim.* **17**: 1517–1528.
- Chakraborty A, Nanjundiah R, Srinivasan J. 2006. Theoretical aspects of the onset of Indian summer monsoon from perturbed orography simulations in a GCM. *Ann. Geophys.* **24**: 2075–2089.
- Chou C, Neelin J, Su H. 2001. Ocean–atmosphere–land feedbacks in an idealized monsoon. *Q. J. R. Meteorol. Soc.* **127**: 1869–1891.
- Colman R, Moise A, Hanson L. 2011. Tropical Australian climate and the Australian monsoon as simulated by 23 CMIP3 models. *J. Geophys. Res.: Atmos.* **116**: D10116. <https://doi.org/10.1029/2010JD015149>.
- Derbyshire S, Beau I, Bechtold P, Grandpeix JY, Piriou JM, Redelsperger JL, Soares P. 2004. Sensitivity of moist convection to environmental humidity. *Q. J. R. Meteorol. Soc.* **130**: 3055–3079.
- Emanuel KA. 1995. The behavior of a simple hurricane model using a convective scheme based on subcloud-layer entropy equilibrium. *J. Atmos. Sci.* **52**: 3960–3968.
- Emanuel KA, David Neelin J, Bretherton CS. 1994. On large-scale circulations in convecting atmospheres. *Q. J. R. Meteorol. Soc.* **120**: 1111–1143.
- Giannini A, Salack S, Lodoun T, Ali A, Gaye A, Ndiaye O. 2013. A unifying view of climate change in the Sahel linking intra-seasonal, interannual and longer time scales. *Environ. Res. Lett.* **8**: 024010. <https://doi.org/10.1088/1748-9326/8/2/024010>.
- Gu G, Adler RF. 2004. Seasonal evolution and variability associated with the West African monsoon system. *J. Clim.* **17**: 3364–3377.
- Haarsma RJ, Selten FM, Weber SL, Kliphuis M. 2005. Sahel rainfall variability and response to greenhouse warming. *Geophys. Res. Lett.* **32**: L17702. <https://doi.org/10.1029/2005GL023232>.
- Holloway CE, Neelin JD. 2009. Moisture vertical structure, column water vapor, and tropical deep convection. *J. Atmos. Sci.* **66**: 1665–1683.
- Hurley JV, Boos WR. 2013. Interannual variability of monsoon precipitation and local subcloud equivalent potential temperature. *J. Clim.* **26**: 9507–9527.
- Janowiak JE. 1988. An investigation of interannual rainfall variability in Africa. *J. Clim.* **1**: 240–255.
- Jin Q, Wei J, Yang ZL. 2014. Positive response of Indian summer rainfall to Middle East dust. *Geophys. Res. Lett.* **41**: 4068–4074. <https://doi.org/10.1002/2014GL059980>.
- Kawamura R, Fukuta Y, Ueda H, Matsuura T, Iizuka S. 2002. A mechanism of the onset of the Australian summer monsoon. *J. Geophys. Res.: Atmos.* **107**: D14. <https://doi.org/10.1029/2001JD001070>.
- Kuang Z. 2010. Linear response functions of a cumulus ensemble to temperature and moisture perturbations and implications for the dynamics of convectively coupled waves. *J. Atmos. Sci.* **67**: 941–962.
- Lau WK. 2014. Atmospheric science: Desert dust and monsoon rain. *Nat. Geosci.* **7**: 255–256.
- Lau WK, Kim KM, Shi JJ, Matsui T, Chin M, Tan Q, Peters-Lidard C, Tao W. 2016. Impacts of aerosol–monsoon interaction on rainfall and circulation over Northern India and the Himalaya Foothills. *Clim. Dyn.* **1**–16. <https://doi.org/10.1007/s00382-016-3430-y>.
- McHugh MJ. 2004. Near-surface zonal flow and East African precipitation receipt during austral summer. *J. Clim.* **17**: 4070–4079.
- Neelin JD, Zeng N. 2000. A quasi-equilibrium tropical circulation model – Formulation. *J. Atmos. Sci.* **57**: 1741–1766.
- Nie J, Boos WR, Kuang Z. 2010. Observational evaluation of a convective quasi-equilibrium view of monsoons. *J. Clim.* **23**: 4416–4428.
- Nolan DS, Zhang C, Chen SH. 2007. Dynamics of the shallow meridional circulation around intertropical convergence zones. *J. Atmos. Sci.* **64**: 2262–2285.
- Parker DJ, Burton R, Diongue-Niang A, Ellis R, Felton M, Taylor C, Thorncroft CD, Bessemoulin P, Tompkins AM. 2005. The diurnal cycle of the West African monsoon circulation. *Q. J. R. Meteorol. Soc.* **131**: 2839–2860.
- Parker DJ, Willetts P, Birch C, Turner AG, Marsham JH, Taylor CM, Kollusu S, Martin GM. 2016. The interaction of moist convection and mid-level dry air in the advance of the onset of the Indian monsoon. *Q. J. R. Meteorol. Soc.* **142**: 2256–2272. <https://doi.org/10.1002/qj.2815>.
- Peixoto JP, Oort AH. 1992. *Physics of Climate*. American Institute of Physics: New York, NY.
- Peyrillé P, Lafore JP. 2007. An idealized two-dimensional framework to study the West African monsoon. Part II: Large-scale advection and the diurnal cycle. *J. Atmos. Sci.* **64**: 2783–2803.
- Privé NC, Plumb RA. 2007. Monsoon dynamics with interactive forcing. Part I: Axisymmetric studies. *J. Atmos. Sci.* **64**: 1417–1430.
- Reed RJ, Norquist DC, Recker EE. 1977. The structure and properties of African wave disturbances as observed during Phase III of GATE. *Mon. Weather Rev.* **105**: 317–333.
- Seager R, Henderson N. 2013. Diagnostic computation of moisture budgets in the ERA-Interim reanalysis with reference to analysis of CMIP-Archived atmospheric model data. *J. Clim.* **26**: 7876–7901.
- Shekhar R, Boos WR. 2017. Weakening and shifting of the Saharan shallow meridional circulation during wet years of the West African monsoon. *J. Clim.* (2017).
- Sherwood SC. 1999. Convective precursors and predictability in the tropical western Pacific. *Mon. Weather Rev.* **127**: 2977–2991.
- Sobel AH, Bellon G. 2009. The effect of imposed drying on parameterized deep convection. *J. Atmos. Sci.* **66**: 2085–2096.
- Sobel AH, Neelin JD. 2006. The boundary layer contribution to intertropical convergence zones in the quasi-equilibrium tropical circulation model framework. *Theor. Comput. Fluid Dyn.* **20**: 323–350.
- Sobel AH, Nilsson J, Polvani LM. 2001. The weak temperature gradient approximation and balanced tropical moisture waves. *J. Atmos. Sci.* **58**: 3650–3665.
- Straub KH, Kiladis GN, Ciesielski PE. 2006. The role of equatorial waves in the onset of the South China Sea summer monsoon and the demise of El Niño during 1998. *Dyn. Atmos. Oceans* **42**: 216–238.
- Sultan B, Janicot S. 2000. Abrupt shift of the ITCZ over West Africa and intra-seasonal variability. *Geophys. Res. Lett.* **27**: 3353–3356. <https://doi.org/10.1029/1999GL011285>.
- Thorncroft CD, Nguyen H, Zhang C, Peyrille P. 2011. Annual cycle of the West African monsoon: Regional circulations and associated water vapour transport. *Q. J. R. Meteorol. Soc.* **137**: 129–147.
- Tompkins AM. 2001. Organization of tropical convection in low vertical wind shears: The role of water vapor. *J. Atmos. Sci.* **58**: 529–545.
- Trenberth KE, Stepaniak DP, Caron JM. 2000. The global monsoon as seen through the divergent atmospheric circulation. *J. Clim.* **13**: 3969–3993.
- Tulich SN, Mapes BE. 2010. Transient environmental sensitivities of explicitly simulated tropical convection. *J. Atmos. Sci.* **67**: 923–940.
- Vinoj V, Rasch PJ, Wang H, Yoon JH, Ma PL, Landu K, Singh B. 2014. Short-term modulation of Indian summer monsoon rainfall by West Asian dust. *Nat. Geosci.* **7**: 308–313.
- Wang B, Ding Q. 2008. Global monsoon: Dominant mode of annual variation in the tropics. *Dyn. Atmos. Oceans* **44**: 165–183.
- Wheeler M, McBride J. 2005. Australian–Indonesian monsoon. In *Intraseasonal Variability in the Atmosphere–Ocean Climate System*, Lau WK-M, Waliser DE. (eds.): 125–173. Springer: Berlin.
- Xie S, Hume T, Jakob C, Klein SA, McCoy RB, Zhang M. 2010. Observed large-scale structures and diabatic heating and drying profiles during TWP-ICE. *J. Clim.* **23**: 57–79.
- Yoneyama K, Parsons DB. 1999. A proposed mechanism for the intrusion of dry air into the tropical western Pacific region. *J. Atmos. Sci.* **56**: 1524–1546.
- Yoshioka M, Mahowald NM, Conley AJ, Collins WD, Fillmore DW, Zender CS, Coleman DB. 2007. Impact of desert dust radiative forcing on Sahel precipitation: Relative importance of dust compared to sea surface temperature variations, vegetation changes, and greenhouse gas warming. *J. Clim.* **20**: 1445–1467.
- Zhang C, McGauley M, Bond NA. 2004. Shallow meridional circulation in the tropical eastern Pacific. *J. Clim.* **17**: 133–139.
- Zhang C, Nolan DS, Thorncroft CD, Nguyen H. 2008. Shallow meridional circulations in the tropical atmosphere. *J. Clim.* **21**: 3453–3470.
- Zhao C, Liu X, Ruby Leung L, Hagos S. 2011. Radiative impact of mineral dust on monsoon precipitation variability over West Africa. *Atmos. Chem. Phys.* **11**: 1879–1893.